# Mechanism of vacancy formation induced by hydrogen in tungsten

Yi-Nan Liu, T. Ahlgren, L. Bukonte, K. Nordlund, Xiaolin Shu, Yi Yu, Xiao-Chun Li, and Guang-Hong Lu

## COLLECTIONS

Paper published as part of the special topic on Chemical Physics, Energy, Fluids and Plasmas, Materials Science and Mathematical Physics

View Online          Export Citation          CrossMark

## ARTICLES YOU MAY BE INTERESTED IN

Solution and Diffusion of Hydrogen in Tungsten
Journal of Vacuum Science and Technology 6, 388 (1969); https://doi.org/10.1116/1.1492699

Diffusion of hydrogen in bcc tungsten studied with first principle calculations
Journal of Applied Physics 107, 113531 (2010); https://doi.org/10.1063/1.3386515

Dissolving, trapping and detrapping mechanisms of hydrogen in bcc and fcc transition metals
AIP Advances 3, 012118 (2013); https://doi.org/10.1063/1.4789547
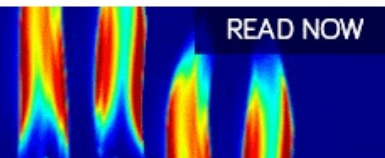
# Mechanism of vacancy formation induced by hydrogen in tungsten

Yi-Nan Liu,[1,2] T. Ahlgren,[2] L. Bukonte,[2] K. Nordlund,[2] Xiaolin Shu,[1] Yi Yu,[1] Xiao-Chun Li,[3] and Guang-Hong Lu[1,a]

[1]*School of Physics & Nuclear Energy Engineering, Beihang University, Beijing, 100191, China*
[2]*Association EURATOM-TEKES, University of Helsinki, Helsinki, PO Box 64, 00560, Finland*
[3]*Institute of Plasma Physics, Chinese Academy of Sciences, Hefei, Anhui, 230031, China*

We report a hydrogen induced vacancy formation mechanism in tungsten based on classical molecular dynamics simulations. We demonstrate the vacancy formation in tungsten due to the presence of hydrogen associated directly with a stable hexagonal self-interstitial cluster as well as a linear crowdion. The stability of different self-interstitial structures has been further studied and it is particularly shown that hydrogen plays a crucial role in determining the configuration of SIAs, in which the hexagonal cluster structure is preferred. Energetic analysis has been carried out to prove that the formation of SIA clusters facilitates the formation of vacancies. Such a mechanism contributes to the understanding of the early stage of the hydrogen blistering in tungsten under a fusion reactor environment. © *2013 Author(s). All article content, except where otherwise noted, is licensed under a Creative Commons Attribution 3.0 Unported License.* [http://dx.doi.org/10.1063/1.4849775]

## I. INTRODUCTION

Defects such as vacancies, grain boundaries and dislocations have significant impact on both the structural and mechanical properties of metals. Among these the vacancy has always drawn intense interest owing to its effects on properties such as diffusion,[1] electrical resistivity[2] and alloy hardening.[3] As one of the intrinsic point defects in metals, the vacancy usually has a quite low concentration of the order of $10^{-4}$ below the melting point under thermal equilibrium conditions.[4,5] External conditions like rapid quenching or high energy particle irradiation can induce vacancy formation in metals, which are usually applied as important ways to investigate the effects of vacancies. In particular, supersaturated vacancies above the equilibrium concentration can be created by irradiation only when the energy transferred to the lattice atom exceeds the displacement threshold.

Along with the establishment of the International Thermonuclear Experimental Reactor (ITER) project, tungsten is considered as one of the most promising candidates for plasma facing materials (PFMs) in ITER and future fusion power plants due to its high melting point and low erosion yield. However, the hydrogen blistering problem in tungsten under plasma irradiation remains a challenging issue, which can reduce the lifetime of the PFMs and the stability of the fusion plasma. Furthermore, the high pressure induced by the hydrogen blistering is responsible for the crack propagation, famous as hydrogen embrittlement which has been examined extensively early in the last century.[6,7] A large body of research is aimed at revealing the mechanism underneath the blistering phenomena. In recent years, hydrogen retention experiments have been carried out to examine the blistering problem.[8–15] The hydrogen retention reaches a maximum around an exposure temperature of 500 K at which

---

[a]Electronic mail: LGH@buaa.edu.cn

temperature the most severe blistering phenomena is also observed, and the blistering disappears at 1000 K.[10] The problem of hydrogen bubble formation in metals has been summarized by Condon and Schober,[16] who attributed the formation mechanism in tungsten to the vacancy clustering.

Several theoretical studies have been carried out, and it is believed that the bubble formation is closely related to the vacancy defect. First-principles calculations suggest that the vacancy in tungsten provides trap sites for hydrogen atoms and one vacancy could at 0 K hold at most 10 hydrogen atoms with one $H_2$ in the center, driven by optimal charge density.[17] This is known as the vacancy trapping mechanism[17,18] which elucidates the bubble formation at the vacancy-type defects such as vacancy and grain boundary[19] where the hydrogen bubbles are observed experimentally.[20] The effect of temperature on the hydrogen accommodation has been studied by the molecular dynamics (MD) simulations which give the decrease of trapped hydrogen number in vacancy as temperature increases.[18] At 300 K, about 6.5 hydrogen atoms are trapped by a monovacancy, while the number decreases to 5 at 900 K. This is basically coincident with the thermodynamic estimation which concludes that the monovacancy can hold up to 5 hydrogen atoms at room temperature.[21] On the other hand, the anisotropic strain is shown to enhance hydrogen solubility which helps the hydrogen bubble growth.[22]

It is known that the equilibrium vacancy concentration in tungsten is as low as $10^{-4}$ even at the melting point.[23] However, the phenomena of hydrogen blistering is indeed observed at the surface of single crystal tungsten under high flux irradiation with quite low energy (not larger than 100 eV).[11–13] Such an energy is certainly insufficient to create new vacancies in tungsten. Since the influence of other defects like grain boundaries is excluded, it still remains an open question how the abundant vacancies essentially required by the vacancy trapping mechanism[16–19] for the hydrogen bubble formation are generated under such a condition and then how hydrogen bubbles are formed.

Different explanations have been provided to explain the experimentally observed hydrogen blistering phenomena in tungsten. Alimov *et. al*[14] believe that the structure change of tungsten plays a crucial role in both the increase of hydrogen retention and blistering, and consider that vacancies are produced by deuterium induced plastic deformation. Shu *et. al*[12,13] explain the experimental results with Fukai's theory of the superabundant vacancies and introduce the deuterium induced local superplasticity during which the vacancies are generated by lowering of vacancy formation energy due to trapping of deuterium. Unfortunately, so far there are no direct experimental or computational results to confirm these explanations. Generally, it is well known that gas bubbles can punch out interstitials and small interstitial dislocation loops if they have started to form in a solid.[24,25] Moreover, the previous MD simulations have found the spontaneous formation of vacancies and interstitials in a pure metal system.[26]

Experimental observations of blistering in single-crystalline tungsten and the vacancy trapping mechanism drive us to consider that the vacancy forms due to the existence of hydrogen atoms retained in tungsten. In this work, we perform classic MD simulations to investigate the probability of the hydrogen induced vacancy formation in tungsten and explore the underlying mechanism, and provide the dynamic process of hydrogen induced vacancy formation with certain hydrogen concentrations. The results help to understand the hydrogen blistering in tungsten as well as in other metals, and thus contribute to the materials design of tungsten based PFMs in future fusion reactors.

## II. COMPUTATIONAL METHODS

The MD simulations using the PARCAS code[27] are used to describe how the vacancies are formed with certain concentrations of hydrogen atoms in tungsten system. We use the self-developed bond-order potential[28] which is suitable to describe the interactions of tungsten-hydrogen system especially in the presence of defects.

The box for tungsten-hydrogen simulation in the bulk consists of 10 unit cells of tungsten atoms in the body-centered cubic (bcc) crystal structure, and periodic boundary conditions are used in all the three dimensions. Hydrogen atoms are randomly distributed in the tetrahedral sites which are the favorable sites for hydrogen in bulk tungsten[29] with the concentrations 20 at.% and 30 at.%. The simulation temperatures range from 600 K to 1500 K. The system is firstly relaxed for 10 ps at 0 K, and then the temperature is slowly increased with the rate of 0.1 K/fs to the desired values and
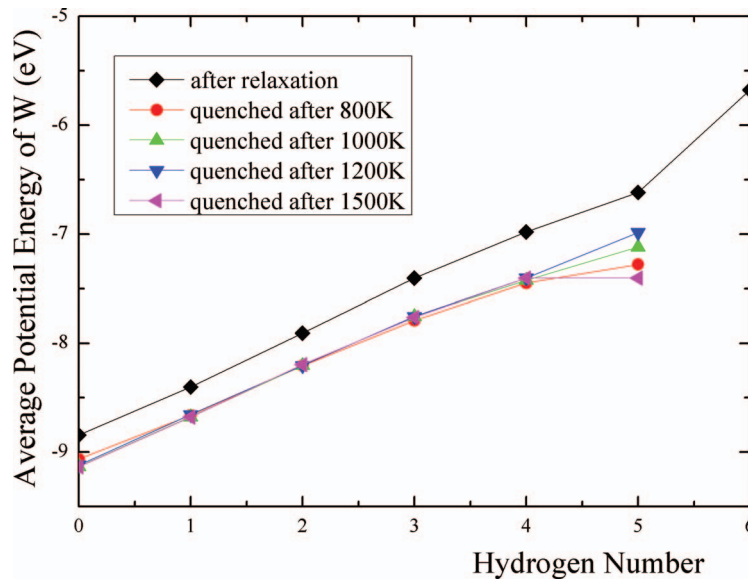
FIG. 1. Average potential energy of tungsten atoms as a function of the surrounding hydrogen number.

kept constant afterwards. The pressure in the system is always kept at zero using Berendsen pressure control.[30] Simulations are performed for at least 7 ns according to different temperatures to make sure the systems reach equilibrium and yield relatively stable vacancy numbers, except in the case of 600 K and 700 K, when the time required to get equilibrium in the system is out of the MD time scale. For the vacancy formation simulations in the surface system, a larger box of $15 \times 15 \times 15$ is used while periodic boundary conditions are applied in the x and y directions with the z direction left as the open surface. The surface systems with hydrogen concentration of 10 at.% and 20 at.% are investigated. The Wigner-Seitz analysis[31,32] is used after each run to get the defect information. This analysis works by counting the number of tungsten atoms in each cell, with the empty cell as a vacancy and the ones with two or more tungsten atoms considered self-interstitial cells. The vacancy cluster analysis is also carried out with the second nearest neighbor (2NN) distance as the cutoff radius. To further investigate the self-interstitial atom (SIA) structures observed during the evolution of tungsten-hydrogen system composed of both the original lattice atoms and the SIAs, initially perfect tungsten systems to which a few SIAs are added are also studied, and energetic analysis on these is carried out.

## III. RESULTS AND DISCUSSION

### A. Vacancy formation induced by hydrogen

We first calculate the average potential energy of tungsten as a function of the surrounding hydrogen number in the tungsten-hydrogen system after reaching equilibrium. The system after molecular static relaxation at 0 K undergoes an annealing procedure with the system first heated to the desired temperatures to get equilibrium and then cooled down to 0 K again. As shown in Figure 1, the average potential energy of tungsten increases with the number of surrounding hydrogens, independent of the elevated temperature. This implies the possibility of vacancy production. Moreover, the average potential energies of tungsten after quenching from different temperatures are almost the same and lower than that from the static relaxation, which indicates that the system becomes more stable after the annealing process.

We then investigate whether vacancies can be generated by the retained hydrogen atoms in tungsten. Via investigating the evolution of the system with different hydrogen concentrations at different temperatures, we indeed found the vacancy formed based on the Wigner-Seitz analysis, confirming our assumption that vacancy can be generated by retained hydrogen.
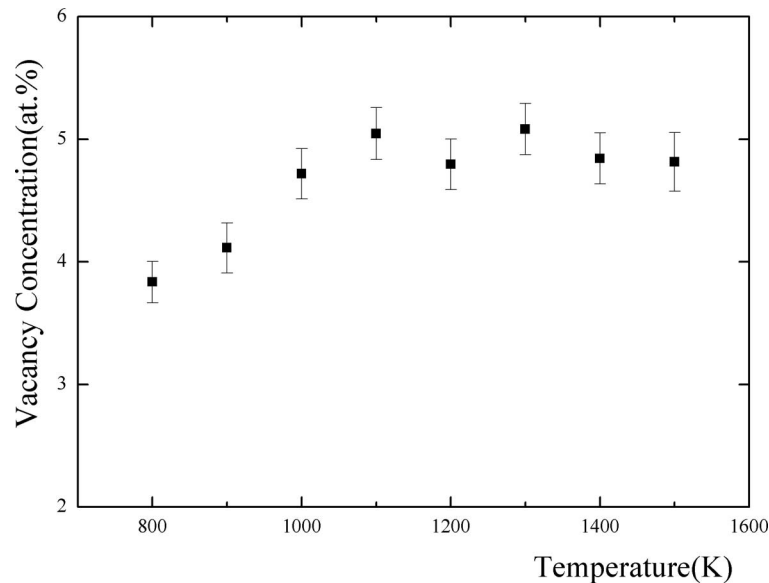
FIG. 2.  Equilibrium vacancy concentration with hydrogen of 30 at.% under different temperatures in the bulk.

The simulations indicate that it is easier for vacancies to form with higher concentration of hydrogen in tungsten. At the concentration of 20 at.%, vacancies can be detected from temperature of 1100 K, while at 30 at.%, vacancies can be detected at the temperature as low as 600 K, within the MD simulation time scale. Meanwhile, with the same hydrogen concentration, vacancies are easier to form at higher temperature. Figure 2 gives the equilibrium vacancy concentration with 30 at.% hydrogen under different temperatures. The vacancy concentrations at the lower temperature region of 800 K and 900 K are lower than those at higher temperatures. However, beyond the temperature of 1000 K, the equilibrium concentration of vacancies remains almost unchanged with temperatures. Under temperatures of 600 K and 700 K, the vacancies can also be detected after running dozens of nanoseconds. The surface simulations show that it is much easier to form vacancies at the surface layers than in the bulk. Vacancies are detected by the Wigner-Seitz analysis at a lower temperature of 500 K with a lower hydrogen concentration of 20 at.% in the surface system. The vacancy cluster analyses of the bulk and surface simulations both yield the existence of vacancy clusters. The divacancies and trivacancies are both detected within the cutoff of the 2NN distance.

Experimentally, the concentration of deuterium in the near surface of single crystal could reach 5 at.%[14] when the fluence increases to $5*10^{23}$ D/m$^2$ after the ion bombardment with flux of $10^{18}$ D/m$^2$s and irradiation energy of 200 eV. It is proved that the actual concentration during the irradiation should be even higher.[33] Thus in this work we choose the hydrogen concentrations of 20 at.% and 30 at.% and mainly deal with the case of 30 at.% hydrogen at 800 K, which is within the blistering regime of temperature in experiment.[10] At a higher temperature, due to the high formation energy and migration barrier of vacancy in tungsten, which are 3.52 eV and 1.81 eV, respectively,[28] its effect on the formation dynamic would be further diminished.

## B.  Hydrogen induced vacancy formation mechanism

Now it is clear that vacancy can form in tungsten with certain hydrogen concentrations. Next we investigate how the vacancy forms due to the presence of hydrogen. It is very interesting that, instead of Frenkel pairs in a perfect lattice, vacancies tend to be formed by the collective movement of several host lattice atoms towards a relatively stable structure of SIAs. Since the vacancy and SIA are generated simultaneously, we should be able to reveal the vacancy formation mechanism by analyzing the related SIA structure.
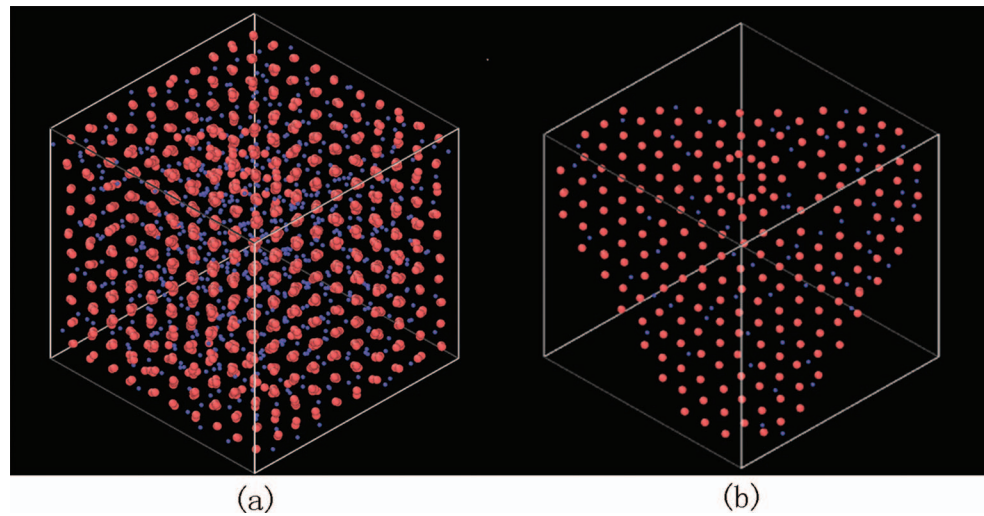
FIG. 3. (a) Hexagonal self-interstitial structure observed after 2 ns at 800 K with 30 at.% hydrogen atoms in tungsten observed from the [111] direction. (b) A clearer picture of this hexagonal cluster demonstrated by the cutting of two (111) hyperplanes.

### 1. Hexagonal structure of self-interstitials

With the formation of vacancies, the SIA clusters characterized by the hexagonal symmetry have been found in tungsten according to the present simulation. For example, such a structure is observed in the tungsten system with 30 at.% hydrogen after running 2 ns at 800 K, as shown in Figure 3(a) with a view from the [111] direction. Figure 3(b) gives a clearer picture of this hexagonal structure consisting of the lattice tungsten atoms and newly induced SIAs. The perfect hexagonal structure exhibited in Figure 3(b) is cut by two parallel (111) hyperplanes with a slice width of 2.8 Angstroms. Since the repeating distance in the [111] direction of bcc tungsten is 2.74 Angstroms, these interstitial atoms are considered to be within one constitutional repeating unit.

More details of the hexagonal cluster are given in Figure 4, pictorially showing the minimal region containing this cluster comprised of thirteen atoms which are amplified according to the atomic hard sphere model. Seen from the [111] view, components of the cluster are separately lying on three layers with only one atom in the center and two hexagons aside, which can also be observed clearly from the lateral view in the lower part of Figure 4(b). Both hexagons referring as A′ and C′, are demonstrated in the insets from the top view and the bond lengths from the atoms of these two hexagons to the very center atom B′ of the cluster are listed in Table I. The original configuration in the same space of the cluster is also given in Figure 4(a), which exhibits the sequential A, B and C layers along the [111] direction of bcc tungsten. Such an original configuration transforms to the hexagonal cluster by each atom of the triangles on layers A and C becoming a ⟨110⟩ dumbbell to form two hexagons on the layers A′ and C′. The hexagon on the lower layer C′ is with the same shape as the superposition of the original A and C layers while the atoms on the the hexagon of layer A′ are rotated to be more closely packed.

To test the stability of such hexagonal SIA clusters, the system shown in Figure 3 is slowly cooled down to 0 K after extracting out the hydrogen atoms. The result shows that both the hexagonal cluster and the detected vacancies still exist in the system, as shown in Figure 5 viewing from the [111] and [100] directions. The two rectangles in Figure 5(b) as a side view seen from the [100] direction are demonstrated to be two hexagonal clusters next to each other but lying on the (-1-11) and (111) planes, respectively. However, these hexagonal clusters vanish if the system in Figure 3 with hydrogen atoms extracted out is first heated to 2000 K and then quenched to 0 K. These results imply that the hexagonal cluster for tungsten is a metastable structure.

To check that the obtained configuration is not an artifact of a single interatomic potential, we also simulated it with two other widely used W potentials, namely the Ackland-Thetford-Nordlund[34]

TABLE I. Bond lengths of the six atoms in layers A′ and C′ to atom B′ in the center of the hexagonal cluster (Angstrom).

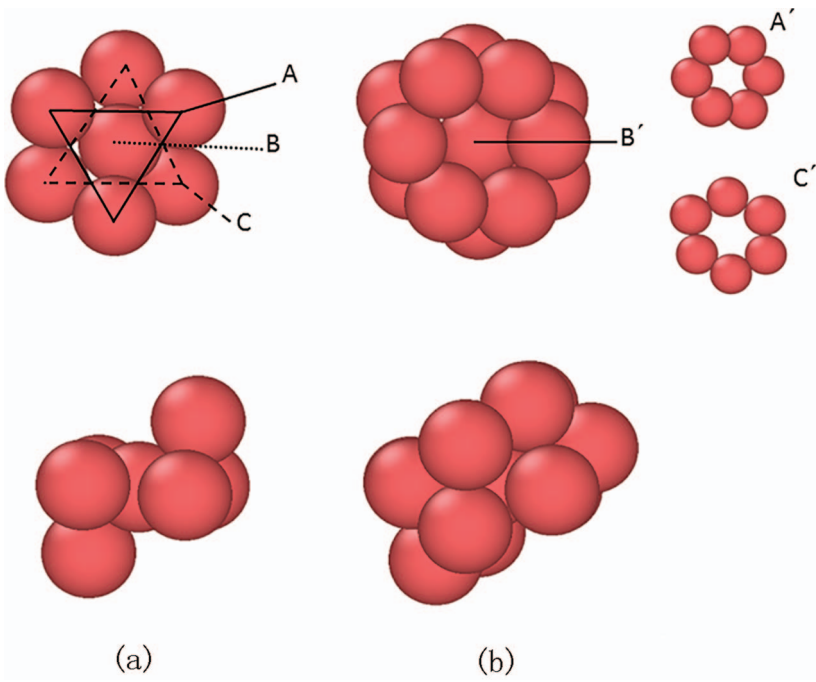| | 1 | 2 | 3 | 4 | 5 | 6 |
|---|---|---|---|---|---|---|
| Layer A′ | 2.96 | 2.79 | 3.08 | 2.90 | 3.01 | 3.09 |
| Layer C′ | 3.08 | 2.92 | 3.12 | 3.12 | 3.06 | 3.29 |



FIG. 4. The top and side views of the hexagonal cluster structure demonstrated in (b) and the original structure in this region shown in (a), composed with one tungsten atom in the center and two pieces of hexagons and triangles, respectively.
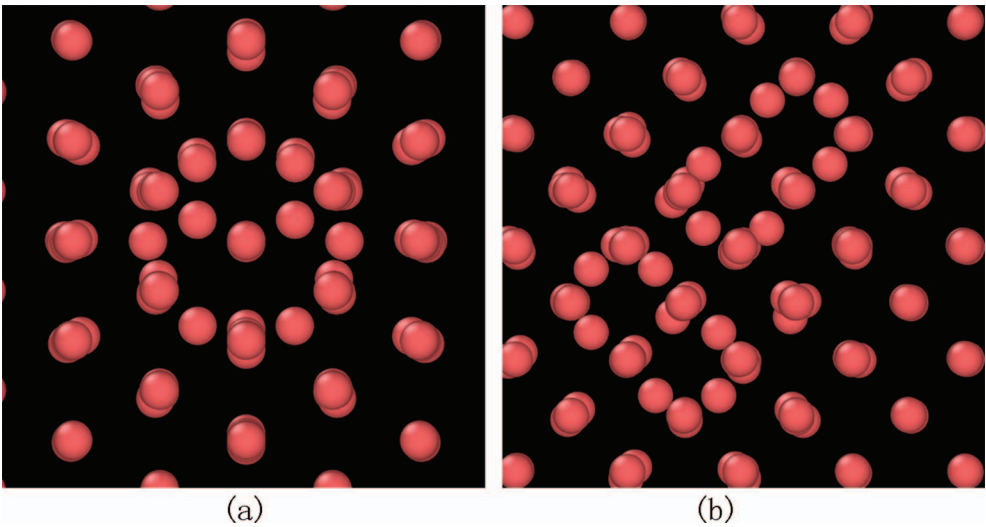


FIG. 5. Configurations of the hexagonal clusters after quenching to 0 K viewed from the [111] and [100] directions, shown as (a ) and (b), respectively.
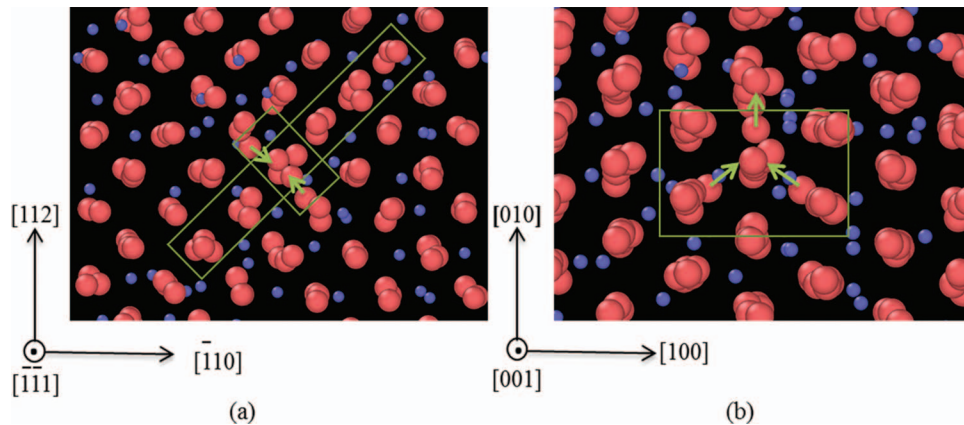
FIG. 6. Linear structure of crowdion formation coming along with the formation of a vacancy from the view of [001] and [-1-11], (a) and (b), respectively.

and the Dudarev-Bjorkas potentials,[35] for the configuration where hydrogen atoms are extracted. We found that the hexagonal cluster (Figure 5) remains in the same configuration after relaxation with these two potentials, which further supports the stability of the cluster.

Such clusters are commonly observed in the tungsten-hydrogen system after reaching equilibrium, and the double-hexagon structure described above is basically the same. Moreover, two clusters next to each other sharing one edge or a vertex also appear occasionally, demonstrating the possible aggregation of the hexagonal clusters.

As to reveal the dynamic process of the vacancy formation, we follow the evolvement of the tungsten-hydrogen system at 800 K and it is shown that the vacancy formation is directly related to the formation of the hexagonal cluster describe above. Half of the hexagonal cluster is observed where three original lattice atoms have been driven by surrounding hydrogen atoms to move and become constituents of the rotated hexagon A′ after running 0.501 ps. At the same time, a vacancy is detected at the original site of the atom which is the first one to rotate. At 0.524 ps, a complete structure of the hexagonal cluster lying on the (111) plane is observed and two vacancies cells are defined where the original atoms have moved to form the cluster. Moreover, one lattice constant away from one of the two detected vacancies, a lattice atom moves to yield another vacancy which is quite stable and persists throughout the simulation after running 0.542 ps. This lattice atom evolves into part of the hexagon C′ of another hexagonal cluster lying on the (-1-11) plane afterwards. Overall, tungsten atoms have been displaced from the original lattice positions and they move collectively to form the hexagonal clusters instead of a single Frenkel pair. Thus the vacancy formation is facilitated by the SIA cluster formation. Most vacancies induced by hydrogen come along with these hexagonal SIA clusters in the bulk simulations.

In the experiments, the observation of small blisters appearing only on grains with nearly (111) surface orientation[13] might be related to the appearance and possible aggregation of these hexagonal clusters lying on the {111} planes observed in the simulations.

### 2. Linear structure of self-interstitials

Besides the hexagonal cluster, a linear crowdion structure is also observed in the tungsten-hydrogen system after running 187.4 ps at 1000 K with the hydrogen concentration of 30 at.% as shown in Figure 6. A vacancy is formed and the corresponding two SIAs detected by the Wigner-Seitz analysis are both in the linear crowdion row as shown in Figure 6(a). Figure 6(b) gives a view from the [-1-11] direction and illustrates the extrusion of the vacancy by two adjacent tungsten atoms moving close along the [1-11] and [-111] orientations. The tungsten atom at the initial lattice position has to move forward along the [111] direction, and becomes a self-interstitial atom. The moving directions of the three tungsten atoms, one originally at the vacancy site and the other two squeezing out the SIAs, are the ⟨111⟩ directions, the easiest ones in tungsten to form a crowdion
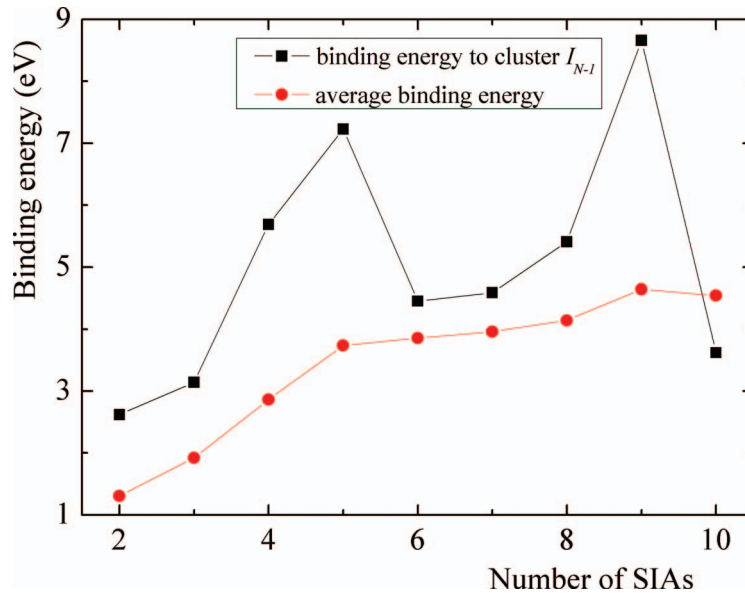
FIG. 7. The binding energy of the $N$th self-interstitial atom to the $I_{N-1}$ structure, and the average binding energy of the $I_N$ structures relative to the single SIA dispersion into the bulk as the increasing number of SIAs.

row[28] as demonstrated with arrows in Figure 6. In this mechanism of vacancy formation, SIAs are not extruded directly by hydrogen atoms, but by the other tungsten atoms nearby instead. However, hydrogen atoms are still the primary cause of vacancy formation. The moves of those two tungsten atoms squeezing out SIAs are driven by the nearby hydrogen atoms, thus this mechanism is an indirect hydrogen-induced vacancy formation mechanism.

## C. Stability of SIA structures in tungsten

### 1. Concentration dependence of the SIA structures

To further investigate the SIA structures closely related to the vacancy formation process, extra $N$ SIAs (with $N$ varying from 1 to 10) are added to the perfect tungsten lattice with the initial positions of SIAs randomly selected. The annealing procedure is applied to the systems, i.e., it is first heated to and kept at various temperatures from 300 K to 2000 K and then cooled down to 0 K to obtain a stable configuration. The structure of $I_N$ containing $N$ extra SIAs with the lowest energy out of several initial distributions is studied and the energetic analysis is carried out as shown in Figure 7. The binding energy of the $N$th SIA to the $I_{N-1}$ structure is calculated according to the following equation

$$E_b^{Nth} = (E(I_{N-1}) + E(I_1)) - (E(I_N) + E(I_0)), \quad (N = 2, 3, \ldots, 10) \tag{1}$$

where $E(I_N)$ stands for the total energy of the system with $N$ extra SIAs. The average binding energy of the SIAs in the $I_N$ structures relative to the single SIA dispersion in the bulk defined as

$$E_b^{aver} = \frac{1}{N}(E(I_N) - E(I_0)) - (E(I_1) - E(I_0)) \quad (N = 2, 3, \ldots, 10) \tag{2}$$

is also demonstrated.

It is clear from the positive binding energy that the SIAs tend to cluster rather than be isolated crowdions, which is the most stable structure of $I_1$. It is shown that the crowdions bundled together along the same ⟨111⟩ direction are the most stable structures for $I_2$ and $I_3$. However, when $N \geq 4$, the hexagonal structures are observed and energetically preferred over the crowdion ensembles. The binding energy of the $N$th SIA to the $I_{N-1}$ structure shows a significant increase while $N$ equals 4, 5, 8 and 9, each case corresponding to a change of the SIA structure. As $N$ equals 4, compared

with the former linear structures, detailed structure analysis gives an SIA cluster containing two hexagons sharing one edge and lying on the (111) and (-11-1) planes, respectively. It is also shown that when $N$ equals 5, 6 and 7, the same structure of three hexagonal clusters all as shown in Figure 4 is observed and the average binding energies are almost the same. Taking $N = 5$ as an example, two clusters lie on the (1-1-1) plane and the third one is on the (11-1) plane connecting those two by sharing edges. It is also worth noticing that the shared edges are both from the rotated hexagons A′ as shown in Figure 4(b). When $N$ equals 8 and 9, much more complicated structures with more than three clusters are formed, thus leading to the increase of the average binding energy.

Considering about the vacancy-SIA pair formation under the condition of inserted hydrogen, our results also show that the energy of the system after extracting out hydrogen and being cooled down to 0 K is much lower than the one with the same amount of separated Frenkel pairs. This result is consistent with the tendency of SIAs to form certain structures instead of isolated crowdions shown in Figure 7. The positive binding energies explain the role of the existing SIAs structures. They behave like a surface here, providing a spot easier to go for the newly created SIAs.

### 2. Temperature dependence of the SIA structures

To test the influence of temperature on the SIA structures, various structures obtained with extra tungsten atoms in pure tungsten are studied after raising the system to different target temperatures. The SIAs with very low concentrations of 1 at.% and 2.5 at.%, corresponding to the cases with $N$ equals 4 and 10 in the system of the last section, respectively, are randomly distributed or put in randomly chosen tetrahedral or octahedral positions simultaneously to study the structures at temperatures of 100 K, 300 K, 600 K, 1000 K and 1500 K. The hexagonal cluster described in Figure 4 is always observed from the ⟨111⟩ views indicating that it is a relatively stable structure for SIAs. Linear structures of SIAs, namely ⟨111⟩ crowdions, appear at the lower SIA concentration of 1 at.% decorated by the hexagonal clusters. However, the fact that the systems with a mixture of crowdions and hexagonal clusters at lower temperatures would yield only the hexagonal clusters at higher temperatures indicating that at higher temperatures, the hexagonal cluster structures are more favorable.

One special case of linear crowdions, namely the interstitial loop structure,[36] transformed from the hexagonal clusters is also observed. During the relaxation at 100 K with 1 at.% extra SIAs in the system, the crowdions along different ⟨111⟩ lattice directions start to orient to the same one and gather together to form an interstitial loop but the sliding of this ensemble gets blocked by a hexagonal cluster. However, when the target temperatures of system are increased to 300 K, 600 K and 1000 K, the interstitial loop breaks through the block of the hexagonal cluster and starts to glide very fast along the aligned [111] direction. Figure 8 illustrates the whole process of the self-interstitial loop overcoming the block from one hexagonal cluster at 300 K from the views of the gliding [111] direction and the [-111] direction in Figure 8(a) and 8(b), respectively.

### 3. Effect of hydrogen on the SIA structures

Based on the above analysis, the temperature and SIA concentration would affect the SIA structures. The simulations with hydrogen in the system also show that the linear structures are barely observed, but the hexagonal ones instead, which implies that the existence of hydrogen atoms also plays a crucial role in determining the configuration of SIAs. It is revealed from the simulations that the SIAs in the linear crowdion region shown in Figure 6 evolve into parts of one hexagonal cluster afterwards, which in a way demonstrates that the cluster structure is more stable with hydrogen in the system. To investigate the effect of hydrogen, 30 at.% hydrogen atoms are added to the interstitial loop structure obtained at 600 K. The results show that the interstitial loop structure is destroyed and hexagonal clusters turn up in the system, which is consistent with the preference of hexagonal structure over linear structure when hydrogen atoms exist in the system.

Since the number of atoms is conserved in a bulk simulation, the vacancy formation is a simultaneous process with the SIA formation. Thus the ways that a vacancy is formed are related to SIA structures such as a hexagonal or linear structure mentioned above, which the tungsten atoms move collectively to form. The preference of hexagonal cluster to linear crowdion in most cases
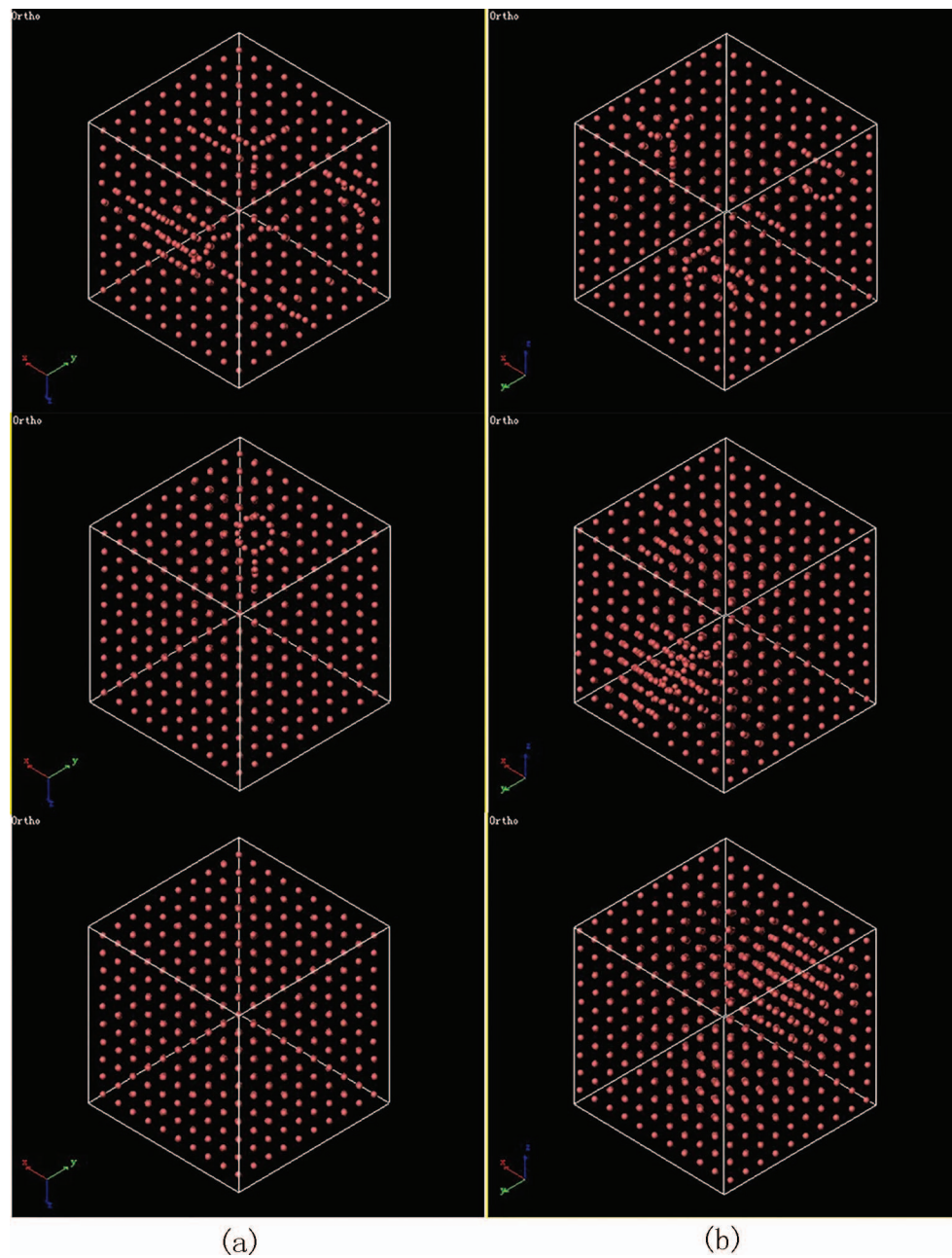
FIG. 8. Formation of self-interstitial loop overcoming the block of hexagonal cluster viewing from the [111] and [-111] directions are shown in (a) and (b), respectively.

is probably due to the existence of hydrogen atoms. Hydrogen atoms block the SIAs continuously moving along one direction and make it easier for the lattice atoms to rotate in a circle, thus forming the hexagonal cluster structure. The fact that the interstitial loop structure as an assembly of linear crowdions grows into the hexagonal clusters after inserting hydrogen atoms, also demonstrates the effect of hydrogen to interstitial cluster formation, i.e. vacancy formation.

While dealing with the vacancy formation induced by hydrogen, as shown in Figure 1, the presence of hydrogen atoms lowers the potential energy of tungsten atoms in the system. Thus, it is concluded that the energy needed to form a vacancy and SIA pair would also be decreased. However, while considering about the required energy for the formation of a vacancy and SIA pair

TABLE II.  Energy required to form a vacancy and to increase the SIA cluster size with the increasing number of surrounding hydrogen atoms (eV).

| (m − 1) SIA to m SIAs | nH | | | |
|---|---|---|---|---|
| | 0H | 1H | 2H | 3H |
| 1 SIA to 2 SIAs | 10.2 | 8.2 | 6.2 | 4.3 |
| 2 SIAs to 3 SIAs | 9.7 | 7.6 | 5.6 | 3.7 |
| 3 SIAs to 4 SIAs | 7.1 | 5.1 | 3.1 | 1.2 |
| 4 SIAs to 5 SIAs | 5.6 | 3.5 | 1.5 | −0.4 |

in the system, it is worth noticing that the number of SIAs obtained simultaneously with vacancies keeps increasing. The energy required to form a vacancy and meanwhile increase the SIA cluster size by one is demonstrated in Table II calculated as

$$E_V^f = \left( E_{V+nH^O} + E_{mSIA} \right) - \left( E_{nH^T} + E_{(m-1)SIA} \right), \tag{3}$$

where the $E_{V+nH^O}$ and $E_{nH^T}$ give the total energies of the systems with $n$ hydrogen atoms occupying the "close to OIS" sites in the vacancy and TIS sites, respectively.[17] The $E_{mSIA}$ and $E_{(m-1)SIA}$ stand for the total energies of the system with $m$ and $(m-1)$ sized self-interstitial clusters, respectively. The energy required to form a vacancy and add an SIA decreases with the increasing number of both the surrounding hydrogen atoms and SIAs, and it turns negative when the lattice tungsten atom is surrounded by 3 hydrogen atoms and 4 SIAs. This would explain the weak influence of temperature on the equilibrium vacancy concentration in Figure 1 since it is characterized by

$$c = c_0 \exp\left( \frac{-H^f}{kT} \right) = c_0 \exp\left( \frac{-E^f}{kT} \right) \exp\left( \frac{P\Delta V}{kT} \right), \tag{4}$$

where $E^f$ is the formation energy calculated in Table II. The formation energy approaches zero at high hydrogen and SIA concentration, thus there could be no dependence on temperature for the equilibrium vacancy concentration at high temperatures. It is well known that the loop punching mechanism works for helium in tungsten to create vacancies.[37] However, unlike the tendency of helium atoms to cluster spontaneously and get pressure accumulation, hydrogen atoms will not form clusters without vacancies. Our work shows that hydrogen atoms tend to modify the tungsten lattice instead and produce hexagonal clusters simultaneously with vacancy formation. We note that the observation of this new defect configuration in bcc tungsten is qualitatively similar to recent observations of several complex low-energy defect structures in bcc Fe.[38,39] In those publications, the hexagonal cluster is one of the tested structures relatively low in energy, while in our work, the hexagonal cluster is directly obtained from the simulation with hydrogen atoms of certain concentration.

## IV. CONCLUSIONS

The hydrogen induced vacancy formation in tungsten, which is considered as the initial step of the hydrogen blistering, has been investigated via classical molecular dynamics simulations. It is shown that vacancies are created due to the presence of hydrogen in tungsten and the vacancy formation mechanism is closely related to the formation of certain self-interstitial structures. In particular, a hexagonal cluster structure with a ⟨111⟩ central axis is observed in tungsten, and it is the primary structure coming along with vacancy formation. Such a hexagonal cluster structure is proved to be stable after being quenched to 0 K, and has also been confirmed with two other interatomic potentials. Besides the hexagonal cluster, a linear crowdion structure is also observed to be associated with vacancy formation, which can evolve into a part of the hexagonal cluster afterwards. Our results demonstrate that hydrogen plays a crucial role in determining the configuration of SIAs, in which the hexagonal cluster structure is preferred. The stability of different self-interstitial structures has been further studied including the hexagonal cluster, linear crowdion, as well as a special case of the linear structure (the interstitial loop) by adding extra self-interstitial atoms into pure tungsten

with different concentration and temperature condition. Energetic analysis has been carried out to prove that the formation of SIA clusters facilitates the formation of vacancies. Such a mechanism of hydrogen induced vacancy formation contributes to the understanding of the early stage of the hydrogen blistering in tungsten under the fusion environment.

## ACKNOWLEDGMENTS

[1] C. P. Flynn, *Point defects and diffusion* (Clarendon Press, Oxford, 1972)
[2] C. Flynn, Physical Review **125**, 881 (1962).
[3] D. Weber, M. Meurtin, D. Paris, A. Fourdeux, and P. Lesbats, Le Journal de Physique Colloques **38**, C7 (1977).
[4] W. D. Callister, *Materials Science And Engineering: An Introduction* (John Wiley & Sons, New York, 2007), p. 82.
[5] P. Ehrhart, *Properties and interactions of atomic defects in metals and alloys* (Springer, Berlin, 1991), p. 88.
[6] J. Hirth, MTA **11**, 861 (1980).
[7] A. R. Troiano, trans. ASM **52**, 54 (1960).
[8] A. C. Rion and J. V. Thomas, Physica Scripta **T94**, 9 (2001).
[9] V. K. Alimov and J. Roth, Physica Scripta **T128**, 6 (2007).
[10] W. M. Shu, K. Isobe, and T. Yamanishi, Fusion Engineering and Design **83**, 1044 (2008).
[11] K. Tokunaga, M. J. Baldwin, R. P. Doerner, N. Noda, Y. Kubota, N. Yoshida, T. Sogabe, T. Kato, and B. Schedler, Journal of Nuclear Materials **337–339**, 887 (2005).
[12] W. M. Shu, E. Wakai, and T. Yamanishi, Nuclear Fusion **47**, 201 (2007).
[13] W. M. Shu, A. Kawasuso, Y. Miwa, E. Wakai, G. N. Luo, and T. Yamanishi, Physica Scripta **T128**, 96 (2007).
[14] V. K. Alimov, J. Roth, and M. Mayer, Journal of Nuclear Materials **337–339**, 619 (2005).
[15] J. P. Roszell, J. W. Davis, and A. A. Haasz, Journal of Nuclear Materials **429**, 48 (2012).
[16] J. B. Condon and T. Schober, Journal of Nuclear Materials **207**, 1 (1993).
[17] Y.-L. Liu, Y. Zhang, H.-B. Zhou, G.-H. Lu, F. Liu, and G. N. Luo, Physical Review B **79**, 172103 (2009).
[18] L. Sun, S. Jin, X.-C. Li, Y. Zhang, and G.-H. Lu, Journal of Nuclear Materials **434**, 395 (2013).
[19] H.-B. Zhou, Y.-L. Liu, S. Jin, Y. Zhang, G. N. Luo, and G.-H. Lu, Nuclear Fusion **50**, 025016 (2010).
[20] R. A. Causey, Journal of Nuclear Materials **300**, 91 (2002).
[21] K. Heinola, T. Ahlgren, K. Nordlund, and J. Keinonen, Physical Review B **82**, 094102 (2010).
[22] H.-B. Zhou, S. Jin, Y. Zhang, G.-H. Lu, and F. Liu, Physical Review Letters **109**, 135502 (2012).
[23] R. W. Siegel, H. Schultz, and K.-D. Rasch, Philosophical Magazine **41**, 91 (1980).
[24] H. Trinkaus, Journal of Nuclear Materials **78**, 189 (1983).
[25] H. Trinkaus and W. G. Wolfer, Journal of Nuclear Materials **122 & 123**, 552 (1984).
[26] K. Nordlund and R. S. Averback, Physical Review Letters **80**, 4201 (1998).
[27] K. Nordlund, M. Ghaly, R. S. Averback, M. Caturla, T. Diaz de la Rubia, and J. Tarus, Physical Review B **57**, 7556 (1998).
[28] X.-C. Li, X. Shu, Y.-N. Liu, F. Gao, and G.-H. Lu, Journal of Nuclear Materials **408**, 12 (2011).
[29] Y.-L. Liu, Y. Zhang, G. N. Luo, and G.-H. Lu, Journal of Nuclear Materials **390–391**, 1032 (2009).
[30] H. J. C. Berendsen, J. P. M. Postma, W. F. van Gunsteren, A. DiNola, and J. R. Haak, The Journal of Chemical Physics **81**, 3684 (1984).
[31] N. D. M. Neil and W. Ashcroft, *Solid State Physics* (Saunders College, Orlando, 1976), p. 73.
[32] N. Juslin, V. Jansson, and K. Nordlund, Philosophical Magazine **90**, 3581 (2010).
[33] G. M. Wright, D. G. Whyte, B. Lipschultz, R. P. Doerner, and J. G. Kulpin, Journal of Nuclear Materials **363–365**, 977 (2007).
[34] Y. Zhong, K. Nordlund, M. Ghaly, and R. S. Averback, Physical Review B **58**, 2361 (1998).
[35] C. Björkas, K. Nordlund, and S. Dudarev, Nuclear Instruments and Methods in Physics Research Section B: Beam Interactions with Materials and Atoms **267**, 3204 (2009).
[36] S. Q. Shi, W. J. Zhu, H. Huang, and C. H. Woo, Radiation Effects and Defects in Solids **157**, 201 (2002).
[37] K. O. E. Henriksson, K. Nordlund, and J. Keinonen, Nuclear Instruments and Methods in Physics Research Section B: Beam Interactions with Materials and Atoms **244**, 377 (2006).
[38] D. Terentyev, T. Klaver, P. Olsson, M. C. Marinica, F. Willaime, C. Domain, and L. Malerba, Physical Review Letters **100**, 145503 (2008).
[39] M. C. Marinica, F. Willaime, and N. Mousseau, Physical Review B **83**, 094119 (2011).